Structural Characteristics of Polyaniline Nanotubes Synthesized from Different Buffer Solutions

Lijuan Zhang, Zoran D. Zujovic, Hui Peng, Graham A. Bowmaker, Paul A. Kilmartin, and Jadranka Travas-Sejdic*

Polymer Electronics Research Centre, Department of Chemistry, University of Auckland, Private Bag 92019, Auckland, New Zealand

Received July 29, 2008; Revised Manuscript Received September 12, 2008

ABSTRACT: Polyaniline (PANI) nanotubes were chemically synthesized from different aqueous buffer solutions: citric acid/phosphate (pH 3 and pH 4 as prepared) and HCl/phthalate (pH 3), beginning with 0.2 M aniline (its presence raises the pH) in the presence of the amino acid alanine and using ammonium persulfate (APS) as the oxidizing agent. For comparison purposes, reactions were also carried out in the absence of any pH controlling agents and from HCl/KCl solution (pH 2). To reveal the effects of the buffer conditions on the morphology and structure of the aniline oxidation products, samples were collected at different times and at different pH values during the polymerization when the pH declines due to acid release from aniline oxidation. The products obtained from the buffer solutions were characterized by SEM, FT-IR, and EPR spectroscopy and compared to the products obtained using "standard" conditions, i.e., without pH buffering. Nanotubes were detected in all of the buffered solutions after 20 h. However, the growth rate and the characteristics of the materials at an early stage of the polymerization process (0 to 5 h) were different for various buffers. In general, the appearance of 860 and 1416 cm^{-1} peaks in FT-IR spectra of the products indicated the presence of nonconducting products generated at the early stages of the reaction and related to roselike morphology. The exception was the aniline oxidation products from citric acid buffer pH 3, which showed a bent tapelike morphology, and its FT-IR spectrum did not show 860 and 1416 cm^{-1} peaks.

Introduction

Polyaniline (PANI) nanotubes have attracted great interest because PANI itself is easy to prepare and has controllable electrical, electrochemical, and optical properties as well as excellent environmental stability.[1] High surface area PANI nanotubes are seen as highly beneficial for potential applications in many areas such as actuators,[2] gas sensors,[3] and biosensors.[4] Many different methods, such as template synthesis,[5] electrospinning,[6] nanofiber seeding,[7] interfacial polymerization,[8] electrochemical polymerization,[9] and self-assembly,[10] have been shown to form PANI nanotubes. Among these methods, the self-assembly method has often been used to prepare PANI nanotubes because this method has the advantage of being simple, and the need for removal of the template postsynthesis is avoided.[11] Although PANI nanotubes have been obtained using the self-assembly method under a variety of conditions, the mechanism of formation of PANI nanotubes is not well understood.[12,13] We have prepared different PANI nanostructures including nanotubes, nanofibers, nanorods, and nanospheres depending upon the different reaction conditions.[14−17] Many different acids including inorganic acids (HCl, H_2SO_4, HBO_4, HF),[18] organic sulfonic acids (β-naphthalenesulfonic acid, camphorsulfonic acid),[19,20] organic carboxylic acids (fatty acids, salicylic acid),[21,22] amino acids (glycine, alanine, leucine, isoleucine, norleucine, and phenylalanine),[23] and polymeric acids (poly(4-styrenesulfonic acid), poly(acrylic acid), and poly(methyl vinyl ether-*alt*-maleic acid))[4] have been used to prepare PANI nanostructures, and it is evident that the pH of the synthesis medium is a key factor controlling the structures obtained. The addition of aniline to a solution has the effect of raising the pH owing to the basic properties of aniline, while the oxidation of aniline releases acid with the effect of lowering the solution pH. Buffering of the polymerization solution has been important, for example, in the enzymatic synthesis of polyaniline[24−27] or for synthesis from a phosphate buffer solution for application in corrosion protection.[28,29] Although these papers report different factors which affect the morphology of polyaniline nanostructured materials, the effects of different buffer solutions to regulate the pH have not previously been considered.

Buffered solutions were used in this study to lessen the effects of the sulfuric acid which is produced during the oxidative polymerization of aniline and to maintain some pH stability in the pH 3−4 range during the first few hours of the reaction. We have examined the evolution of the morphologies and structural characteristics of the products during the reaction using SEM, FT-IR, and EPR spectroscopies and explored the formation of nanotubes from the different buffered (or nonbuffered) solutions. The mechanism of nanotube formation is currently being investigated and will be reported in a subsequent communication.

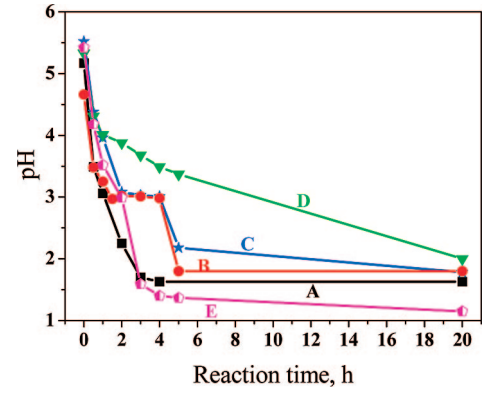

Figure 1. Variation of the pH with the aniline oxidation time using APS in the presence of alanine: (A) in the nonbuffered solution, (B) with pH 3 (citric acid/phosphate) buffer, (C) with pH 3 (HCl/phthalate) buffer, (D) with pH 4 (citric acid/phosphate) buffer, (E) in the pH 2 (HCl/KCl) solution.

* Corresponding author: Tel +64 9 373 7599ext 85876; Fax +64 9 3737422; e-mail j.travas-sejdic@auckland.ac.nz.

10.1021/ma801728j CCC: $40.75
Published on Web 10/22/2008

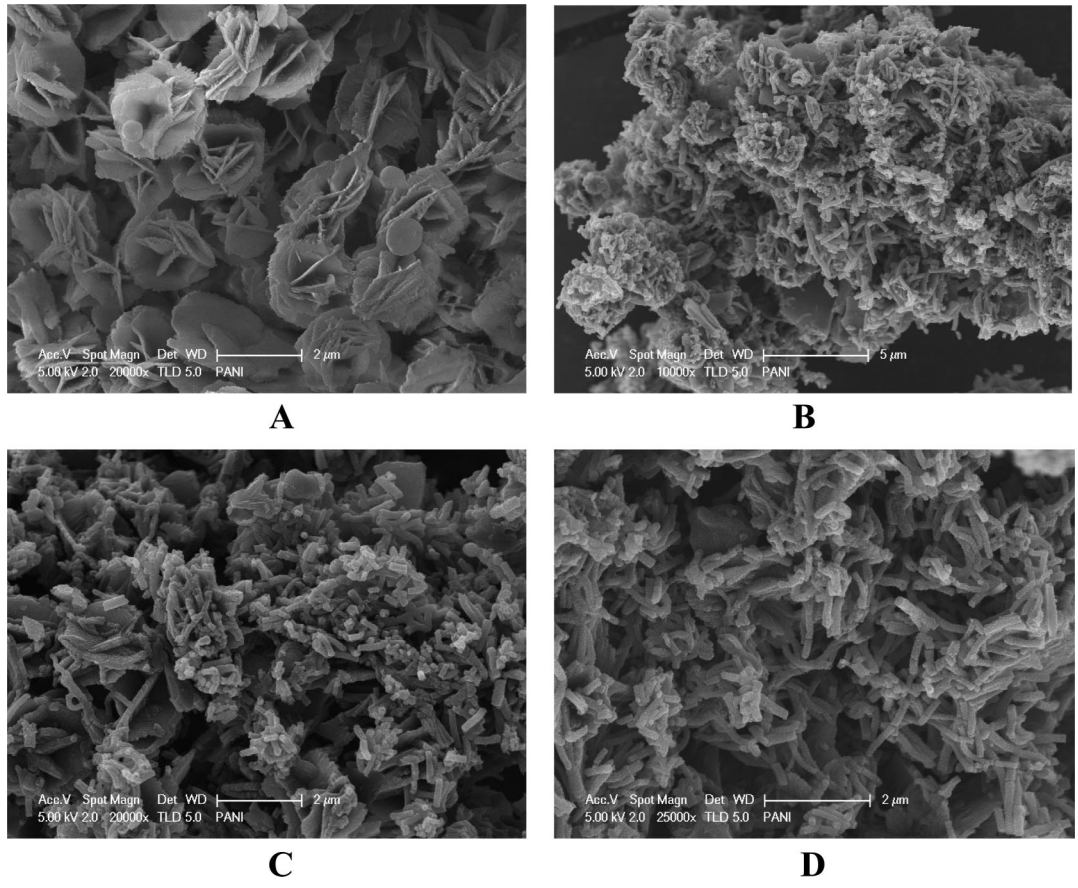

Figure 2. SEM micrographs of the aniline oxidation products synthesized using APS in the presence of alanine in the nonbuffered solution, obtained after 1 h (A), 3 h (B), 5 h (C), and 20 h (D) reaction time.

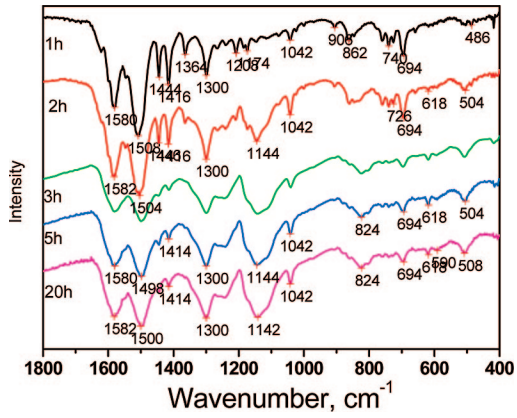

Figure 3. FT-IR spectra of aniline oxidation products synthesized with APS in the presence of alanine in the nonbuffered solution, obtained after 1, 2, 3, 5, and 20 h reaction time.

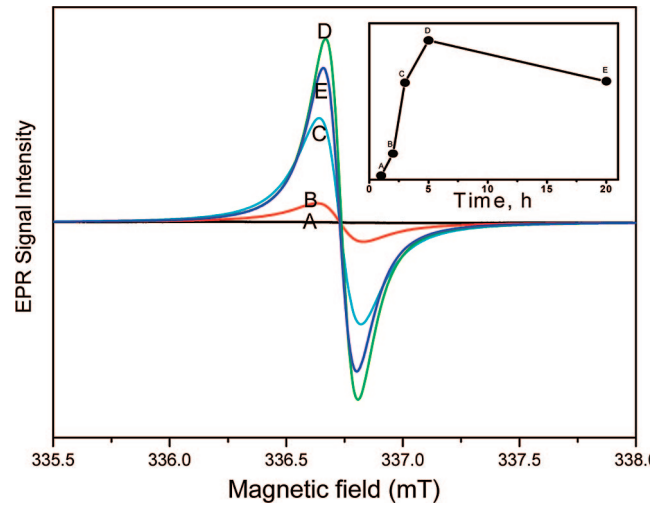

Figure 4. EPR spectra of aniline oxidation products obtained in the nonbuffered solution, obtained after 1 h (A), 2 h (B), 3 h (C), 5 h (D), and 20 h (E) reaction time.

Experimental Section

Materials. Aniline and ammonium persulfate ($(NH_4)_2S_2O_8$, APS) were obtained from Aldrich Chem. Co. Aniline was distilled under reduced pressure and stored in the dark under nitrogen. The amino acid alanine was purchased from Sigma.

Buffers. The pH 3.0 citric acid/phosphate aqueous buffer solution[33] was prepared by mixing 79.45 mL of 0.1 M citric acid and 20.55 mL of 0.2 M dibasic sodium phosphate (Na_2HPO_4). The pH 4.0 citric/phosphate aqueous buffer solution[33] was prepared by mixing 61.45 mL of 0.1 M citric acid and 38.55 mL of 0.2 M dibasic sodium phosphate (Na_2HPO_4). The pH 3.0 phthalate/HCl aqueous buffer solution was prepared by mixing 71.2 mL of 0.2 M potassium hydrogen phthalate ($HOOCC_6H_4COOK$) and 28.8 mL of 0.2 M hydrochloric acid (HCl).

A KCl/HCl solution of pH 2.0 was prepared by mixing 25 mL of 0.2 M potassium chloride (KCl) and 6.5 mL of 0.2 M hydrochloric acid (HCl).

The pH value of the resulting solutions was confirmed using a Sartφrius PB-11 pH meter.

Synthesis. PANI nanotubes were synthesized by dissolving aniline (0.182 mL, 2 mmol) and amino acid alanine (0.0356 g, 0.4 mmol) in 10 mL of reaction solution (Milli-Q water or buffer solution) at room temperature. The reaction solution was cooled in

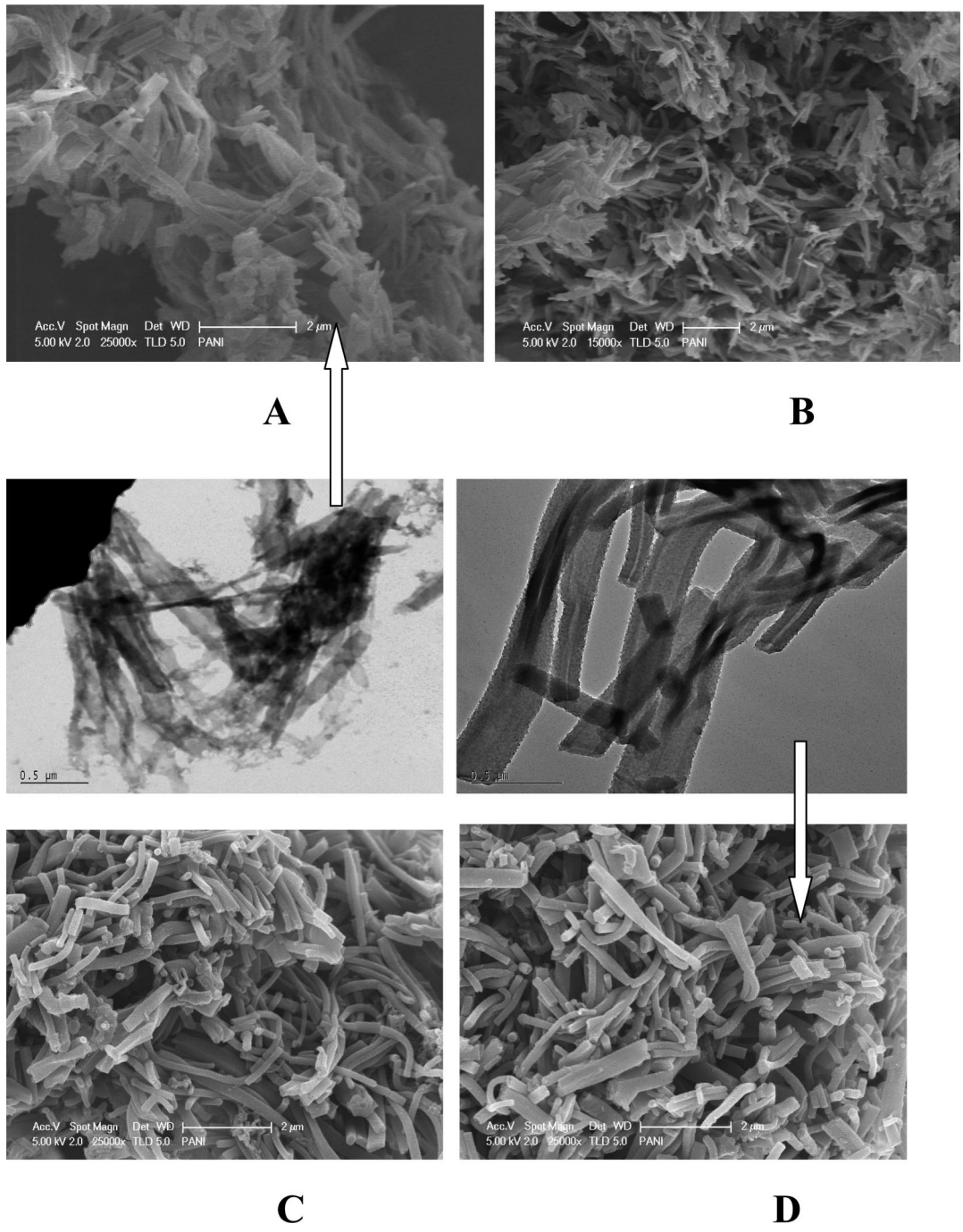

Figure 5. SEM micrographs of the aniline oxidation products synthesized using APS in the presence of alanine in the pH 3 buffered solution (citric acid/Na_2HPO_4 buffer), obtained after 1 h (A), 3 h (B), 5 h (C), and 20 h (D) reaction time. TEM micrographs for the samples taken after 1 and 20 h are indicated by arrows.

a refrigerator at 3 °C for 30 min, after which 5 mL of a precooled solution (Milli-Q water or buffer solution) of 0.4 M APS was added, to give an initial concentration of aniline = 0.133 M, alanine = 0.027 M, and APS = 0.133 M. In order to reveal the morphology and the nature of the products at several stages, the reaction was stopped at the different times (1, 3, 5, and 20 h). The obtained samples were filtered, and the precipitate was washed with water several times.

SEM and TEM Characterization. The morphology of the products was investigated using a Philips XL30S field emission scanning electron microscope (SEM) and a JEOL TEM-2010 transmission electron microscope (TEM). The samples for SEM were mounted on aluminum studs using adhesive graphite tape and sputter-coated with platinum before analysis. Samples for TEM measurements were dispersed on microgrids copper coated on a carbon support film.

Spectroscopy. Infrared spectra in the range 400−4000 cm^{-1} were measured on pellets made with KBr by means of a Perkin-Elmer 1600 FT-IR spectrophotometer, taking 10 scans at a resolution of 4 cm^{-1}. Electron paramagnetic resonance (EPR) spectra were recorded for powder samples in standard quartz EPR tubes using a JEOL JES-FA200 EPR spectrometer. The mass of all the samples was fixed at 2.86 mg, and the experiments were run under ambient conditions.

Conductivity. The room temperature conductivity of samples was measured by a standard four-probe method using a Jandel Model RM2 instrument. The samples were pelletized to a diameter of 1.5 cm and a thickness of 0.6 mm using a vacuum press at 8 tons for 5 min.

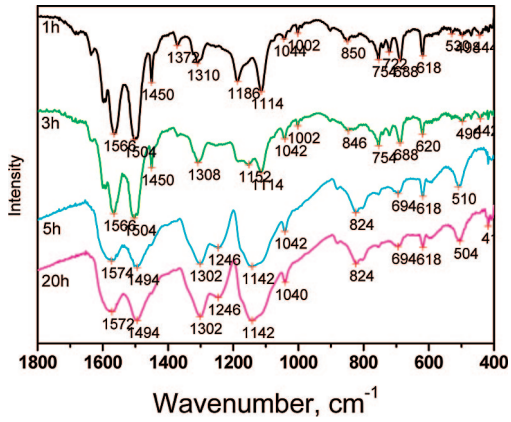

Figure 6. FT-IR spectra of aniline oxidation products synthesized with APS in the presence of alanine in the pH 3 buffered solution (citric acid/Na_2HPO_4 buffer), obtained after 1, 3, 5, and 20 h reaction time.

Results and Discussion

Figure 1 shows the evolution of pH in the reaction mixture during the oxidative polymerization of aniline in the presence of the buffered (B−D) and nonbuffered (A, E) solutions. In all cases, the initial pH was around 7−8 after the addition of aniline but before adding the APS oxidant solution. After the addition of APS, due to the oxidation of aniline and release of protons, the pH dropped rapidly to approximately 5−5.5 and reached pH 3−4 after 1 h of the reaction for all solutions. The pH then continued to decline at different rates for various solutions, reaching the pH range 1.2−2 after 20 h. By that time a black-green precipitate of PANI was formed. The initial fall in pH is due to protonation of the aniline; if x is the extent of reaction ($0 \leq x \leq 1$), then the amount of unpolymerized aniline is $2.0(1 - x)$ mmol and the amount of H^+ produced by the polymerization is $4.0x$ mmol. Thus, the aniline ceases to consume the protons produced when $2.0(1 - x) = 4.0x$, i.e., when $x = 0.33$ (the reaction is 33% complete, which occurs after ca. 2 h). For the potassium hydrogen phthalate buffer, the pH remains at 3.0 until all of the hydrogen phthalate has been converted to phthalic acid, which occurs theoretically at $x = 0.55$ (the reaction is 55% complete experimentally, after ca. 4 h). Beyond this point the buffer is ineffective, and the pH decreases steadily as the polymerization reaction continues to produce protons.

1. Aniline Oxidative Polymerization in the Nonbuffered/Nonacidified Solution. The samples obtained in the nonbuffered solution at reaction times less than 2 h were yellowish-brown, while the samples collected at times longer than 3 h were dark green in color. The SEM images of the samples collected during the reaction in the nonbuffered solution at the different reaction times are shown in Figure 2. The morphology of the sample collected after 1 h of the reaction was "flakelike" or roselike (Figure 2A) (note that pH at that stage was around 3). The first tubular morphologies had been already formed when the reaction time reached 3 h (Figure 2B) when the pH had declined to around 1.5. It appears that the nanofibers grow onto the flakelike structures. After this the pH remained at approximately the same value, but the nanotubular morphologies became more abundant (Figures 2C,D).

FT-IR spectra from the samples taken at different polymerization times during the reaction in the solution without added buffer are shown in Figure 3. As the reaction progressed, there were significant changes in the FT-IR spectra. The peaks at 1582 and 1508 cm^{-1},[30] ascribed to C=C stretching deformation of quinoid and benzenoid rings, shifted to slightly lower frequencies as the reaction progressed. Also, there was a band due to an aromatic stretching vibration at 1444 cm^{-1}. The presence of a group of bands at 1416, 1208, and 1136 cm^{-1} has previously been assigned to the symmetric stretching of phenazine rings which may be formed in small amounts at the beginning of the reaction.[12] Bands at 1364 and 1300 cm^{-1} are attributed to C−N stretching vibrations. The band at 1141 cm^{-1} is assigned to the doped state of PANI, and an increase in the intensity of this peak suggests that the doping level increases during the polymerization. The peak at 1042 cm^{-1} could be assigned to sulfonate groups due to the incorporation of sulfate or hydrogen sulfate as counterions.[12]

The peak at 860 cm^{-1} is characteristic of polysubstituted aniline rings and indicates the presence of *ortho* coupling during the oxidative polymerization. On the other hand, the band at 828 cm^{-1} suggests the presence of *para* disubstituted rings. The bands at 694 and 758 cm^{-1} are characteristic of monosubstituted aromatic rings, assigned as aniline oligomers,[30,31] and their intensity declined as the polymerization continued and with the expected increase in the chain length of the aniline oligomers.

The FT-IR spectra indicate that the flakelike morphology in the sample after 1 h could be partly produced by the presence of phenazine-like, highly branched structures (peak at 1416 cm^{-1}). It has been shown that the electrochemical polymerization of 2-aminodiphenylamine (*ortho*-) dimers produces "flaky" structures, while polymerization of 4-aminodiphenylamine (*para*-) dimers leads to more fiberlike structures.[32]

During the polymerization reaction, the peak at 740 cm^{-1} related to the vibrations of monosubstituted benzene ring and the peak at 860 cm^{-1} due to polysubstituted benzene rings were replaced by the peak at 824 cm^{-1} corresponding to the out-of-plane deformation of C−H in the 1,4-disubstituted benzene ring.[33] This is in line with the fact that at longer reaction times the 1300 cm^{-1} band assigned to the C−N stretching of secondary aromatic amine (π-electron delocalization) became much broader, and the peak at 1144 cm^{-1}, associated with the $-NH^{\bullet+}=$ structure, appeared.[12] Also, the peak at 1416 cm^{-1} decreased in intensity, and the bands at 1208 and 1136 cm^{-1} disappeared during the polymerization. These changes indicate increased delocalization of the electrons along the polymer chains due to a para-coupling, elongation of the polymer, and an increase in doping level. This further means that the aniline oxidation products change from an insulator state, the (oligomeric) flakelike structures,[32] to conducting forms of PANI nanotubes. Figure 4 presents the EPR spectra of the samples obtained in the nonbuffered solution. The intensity of the EPR signal increased as the reaction continued up until 5 h and then decreased for the product at 20 h (inset in Figure 4). This is in accordance with the expectation that at the end of the reaction, and with more advanced oxidation of the polymer, the product may contain a higher proportion of spinless bipolarons, while at earlier stages of the reaction mainly polarons are formed.

The results from SEM, FT-IR, and EPR suggest that the growth of the nanotube morphology coincides with the formation of conducting PANI polymer chains.

2. Aniline Oxidative Polymerization in the Buffered Solutions and an Acidified Solution. In order to investigate the effect of the buffers on the morphology and structure of the aniline oxidation products and PANI nanotubes, the polymerization was carried out in aqueous buffer solutions at pH 3 and pH 4 and in an acidified solution (pH 2 initially). The changes in pH values for the reactions in buffered solutions are shown in Figure 1 (curves B−D). It can be seen that, in spite of using the buffers, the initial pH was almost the same as when the buffer was not used (pH ~5−6), and only afterward from 1 to 4 h did the buffering action of the solution become apparent.

2.1. pH 3 Solution (Citric Acid/Na_2HPO_4 Buffer). When this buffer was used, the pH of the reaction solution dropped to pH

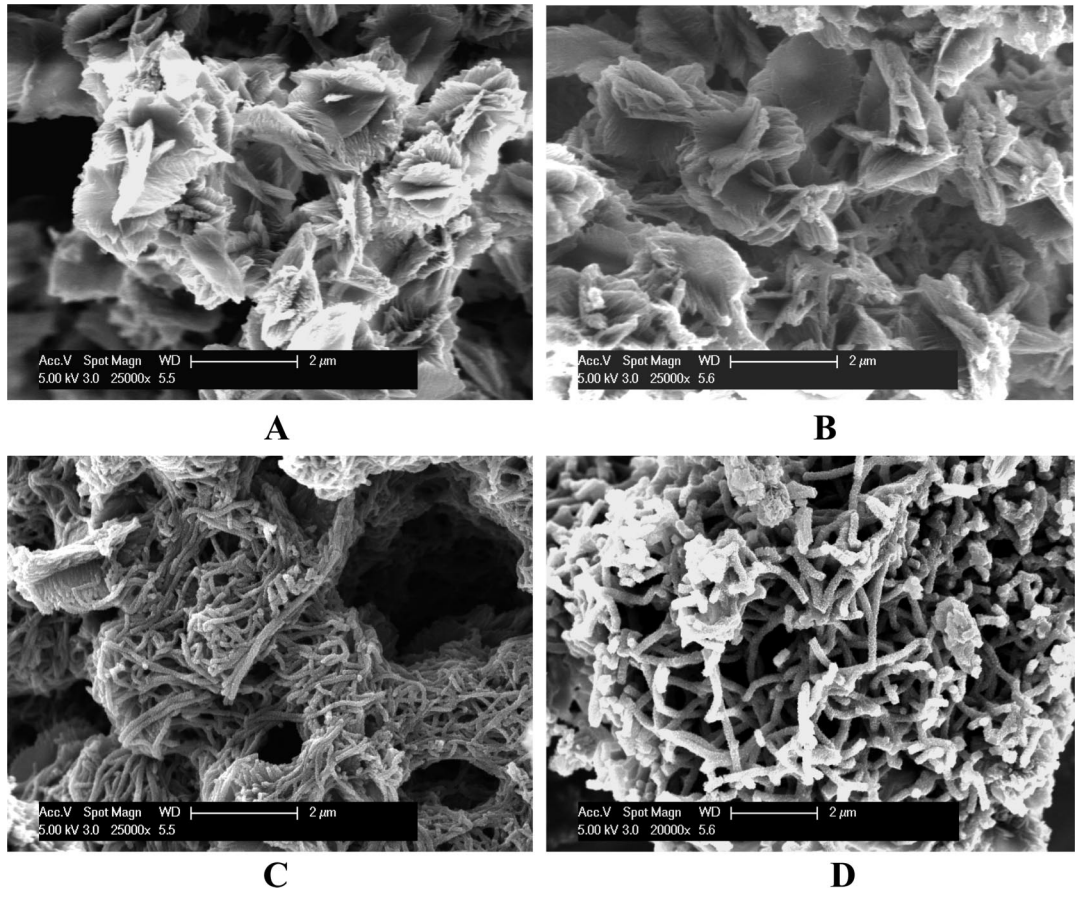

Figure 7. SEM micrographs of the aniline oxidation products synthesized using APS in the presence of alanine in the pH 3 buffered solution (HCl/phthalate buffer), obtained after 1 h (A), 3 h (B), 5 h (C), and 20 h (D) reaction time.

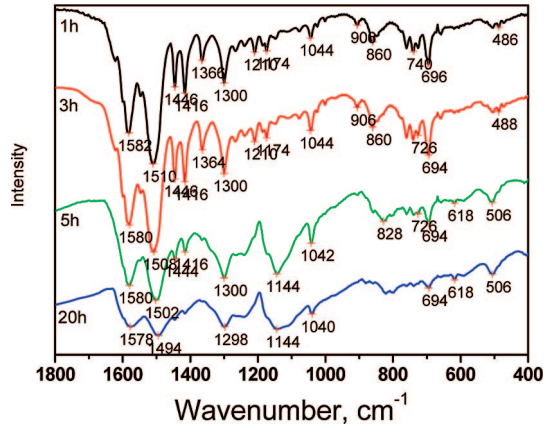

Figure 8. FT-IR spectra of aniline oxidation products synthesized with APS in the presence of alanine in the pH 3 buffered solution (phthalate/HCl buffer), obtained after 1, 3, 5, and 20 h reaction time.

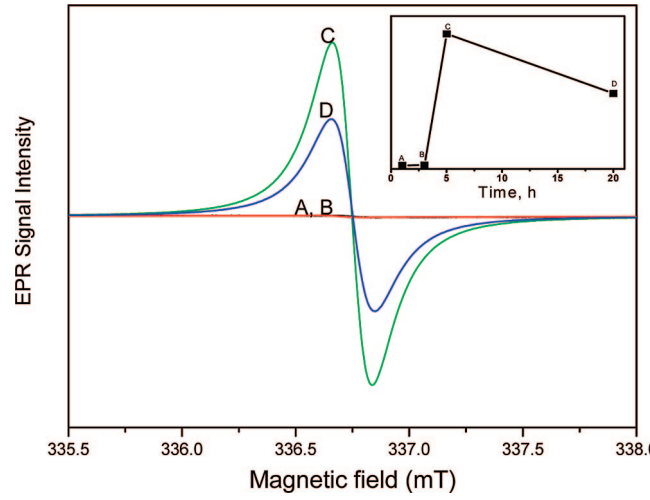

Figure 9. EPR spectra of aniline oxidation products synthesized with APS in the presence of alanine in the pH 3 buffered solution (phthalate/HCl buffer), obtained after 1 h (A), 3 h (B), 5 h (C), and 20 h (D) reaction time.

~ 3 after an hour where it remained for another 3 h, demonstrating the good buffering ability of the HCl/phatlate buffer. After 5 h the pH dropped to around 1.8 as the buffering capacity of the buffer was exhausted and stayed at this value for the remainder of the reaction. The samples obtained in this buffer solution at the reaction times less than 4 h were yellowish-brown, while the samples collected at times longer than 5 h were dark green in color. The morphologies obtained for samples taken at different reaction times are shown in Figure 5. As can be seen from the SEM image taken after 1 h, bent tapelike structures were formed which was confirmed by means of TEM (see Figure 5A and arrow). At that reaction time the pH was around 3, very similar to the pH for the sample obtained in nonbuffered solution. The difference in the morphology of the samples after 1 h indicates that in the first stage of the reaction not only the pH but also other factors, such as the presence of added salts, could influence nanotube formation. The tapelike structures still prevailed after 3 h (see Figure 5C), while after 5 h when the pH dropped to 1.8, nanotubes were prevalent (Figure 5D). The nanotube morphology continued to form for up to 20 h, as confirmed by TEM (Figure 5D).

FT-IR spectra of the samples taken at the different reaction times are presented in Figure 6. The spectra after 1 h (pH =

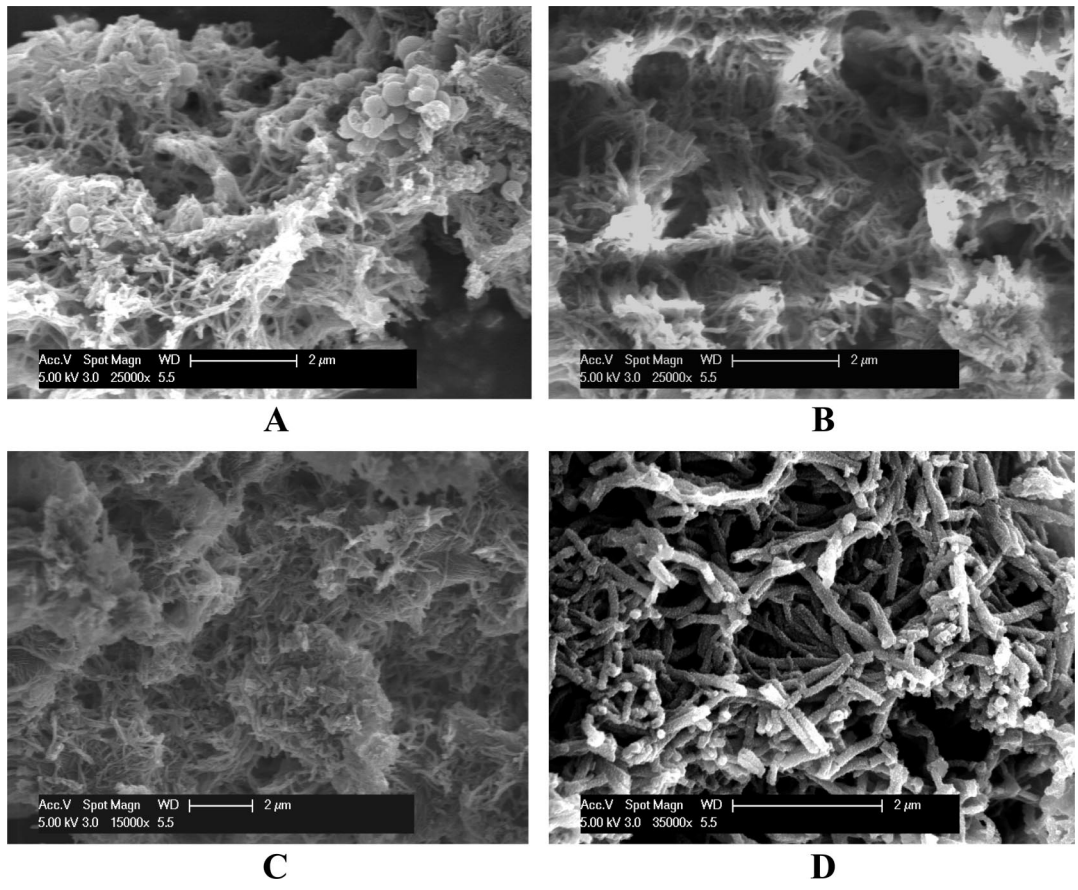

Figure 10. SEM micrographs of the aniline oxidation products synthesized using APS in the presence of alanine in the pH 4 buffered solution (citric acid/Na_2HPO_4 buffer), obtained after 1 h (A), 3 h (B), 5 h (C), and 20 h (D) reaction time.

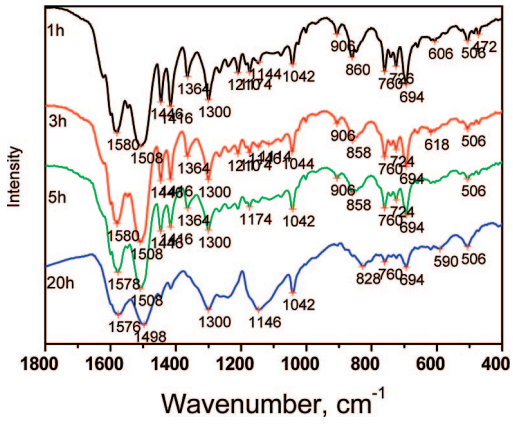

Figure 11. FT-IR spectra of aniline oxidation products synthesized with APS in the presence of alanine in the pH 4 buffered solution (citric acid/Na_2HPO_4 buffer): after 1, 3, 5, and 20 h reaction time.

3.2) and 3 h (pH = 3.0) were very similar and resemble the spectra expected for aniline oligomers.[12,34] A significant difference is the absence of the peaks at 1416, 1208, and 1136 cm^{-1} for the samples obtained in the citric acid/Na_2HPO_4 buffer, the peaks which have previously been assigned to phenazine-like units.[12] These units are attributed to the initial branched structures and were observed in the products with a flakelike morphology.

The absence of the peaks at 1416, 1208, and 1136 cm^{-1} and the fact that the tapelike structures prevail in the samples after 1 and 3 h could suggest that the missing peak belongs to phenazine-like units which are required in the formation of the roselike structures (Figure 2A). When the pH dropped to 1.8 (after 5 h), the FT-IR spectra are indicative of a typical polyaniline structure as the morphology became nanotubular. The emergence of the peak at 1142 cm^{-1} at the longer reaction times confirms that the nanotubes are partially conductive, in line with the appearance of the peak at 824 cm^{-1} which confirms para-coupling. A small peak at 1700 cm^{-1} (seen in Figure 6A) could originate from citric acid, but it is not obvious in the samples obtained at later stages of the reaction.

2.2. pH 3 Solution (HCl/Phthalate Buffer). We have performed further experiments with a pH 3 HCl/phthalate buffer. Our motivation was to see whether the pH dependence or the nature of the buffer is more critical in driving the formation of the initial structures. After 1 h the pH dropped to 4 (see Figure 1). This was somewhat higher than for the citric acid/Na_2HPO_4 buffer where the pH after 1 h was around 3.3. After 3 h the pH reached 3 and remained at this value up to 4 h when it started to drop to around 2.2, before decreasing to 1.8 after 20 h. With some differences, the pH dependence of phthalate/HCl buffer was very similar to the pH dependence of citric acid/Na_2HPO_4 buffer (see Figure 1).

Figure 7 shows the SEM images of the samples collected at the different reaction times using the phthalate/HCl buffer. One can see that the products have a roselike morphology after both 1 (pH 4) and 3 h (pH 3) (Figure 7A,B). After 5 h the pH decreased to 2.3, and the morphology of the product changed to a mainly nanofibrous one (Figure 7C). As the pH slowly decreased toward pH 1.8 and after 20 h the nanotubular morphology dominated (Figure 7D).

FT-IR spectra of the samples taken at the different reaction times are shown in Figure 8. As in the previous experiments the FT-IR spectra of nonfibrous morphologies after 1 and 3 h show characteristics of aniline oligomers. The presence of the peak at 860 cm^{-1} confirms the presence of para-substituted aniline rings. Also, the peak at 1416, 1208, and 1136 cm^{-1}

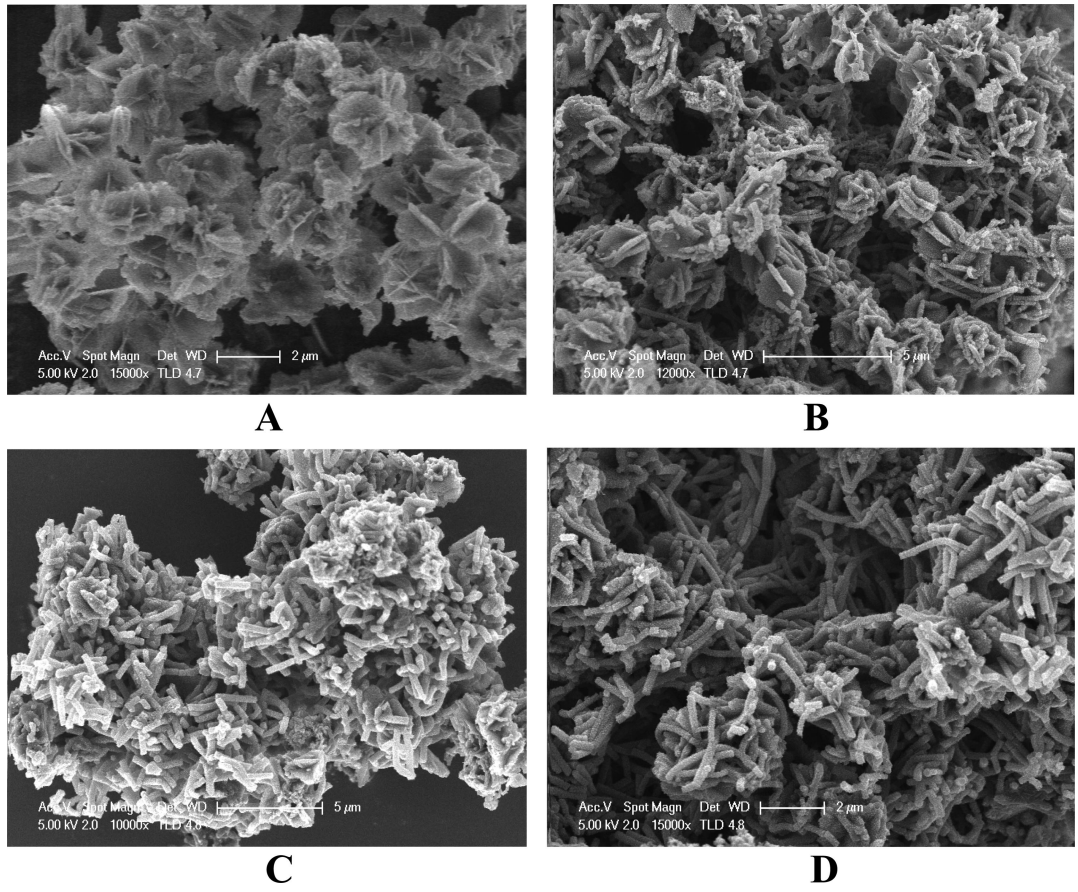

Figure 12. SEM micrographs of the aniline oxidation products synthesized using APS in the presence of alanine in the pH 2 solution (added HCl/KCl), obtained after 1 h (A), 3 h (B), 5 h (C), and 20 h (D) reaction time.

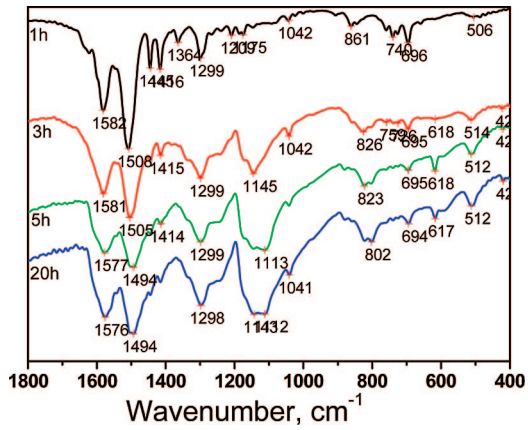

Figure 13. FT-IR spectra of aniline oxidation products synthesized with APS in the presence of alanine in the pH 2 solution (added HCl/KCl), obtained after 1, 3, 5, and 20 h reaction time.

reappears which corresponds to the presence of structures with a roselike morphology in this buffer system.

According to the previous FT-IR experiments (see Figure 8), these cross-linked structures associated with the bands at 1416, 1208, and 1136 cm^{-1} could involve phenazine-like units. As the reaction continued, the pH dropped, and after 5 h the FT-IR spectra showed characteristics of standard polyaniline and SEM images again showed a nanotubular morphology. As in the case of nonbuffered solution, the EPR spectra (see Figure 9A,B) show that the polarons are not present in the branched structures after 1 and 3 h and that the sample became conductive after 5 h (Figure 9C). The difference between the SEM images and FT-IR for samples obtained with two the different buffer systems suggests that not only pH affects the initial morphology but also the presence of different acids can be a very important factor.

2.3. pH 4 Solution (Citric Acid/Na_2HPO_4 Buffer). The evolution of the pH during the reaction time for aniline oxidative polymerization in the pH 4 buffered solution is shown in Figure 1. The pH dropped steeply to around 4 after 1 h of reaction time and then decreased more slowly toward pH 2 after 20 h. The SEM micrographs of the samples taken after 1, 3, 5, and 20 h are shown in Figure 10.

As can be seen after 1 h (pH 4.3), the sample shows several types of morphologies: flakes mixed with fibrous and spherical structures. After 3 and 5 h the pH dropped to 3.75 and 3.4, respectively, and the whole structure was more fibrous-like. After 20 h, when the pH reached 2, nanotubes and nanofibers became the dominant structures. The corresponding FT-IR spectra are shown in Figure 11. The spectra after 1, 3, and 5 h have features typical of cross-linked aniline oligomers (peaks at 1416 and 860 cm^{-1} and a peak at 695 cm^{-1}, which are characteristic of monosubstituted aniline rings). After 20 h when the pH dropped to around 2 the spectrum exhibits characteristics of standard polyaniline.

2.4. An Acidified pH 2 Solution (Added HCl/KCl). In the case when an acidified (pH 2) solution was used (Figure 1E), the pH dropped after 3 h to 1.5 in a similar manner to the reaction without added buffers (see Figure 1A). After that time the pH dropped more steadily and after 20 h finally reached a value around pH 1. The morphologies of the samples taken at different reaction times are shown in Figure 12.

The evolution of the morphology during the reaction time in the acidified pH 2 solution (Figure 12) was very similar to the one obtained for the nonbuffered solution (see Figure 2). The

characteristic flakelike morphologies were present in the sample after 1 h while the nanotubular morphologies appeared after 3 h. These became more dominant as the reaction continued, and the sample after 20 h showed a prevalence of nanotubes.

FT-IR spectra of the samples taken at the different reaction times are shown in Figure 13. As in the previous experiments, the FT-IR spectra of the nonfibrous morphologies after 1 h showed characteristics of aniline oligomers. The presence of the peak at 860 cm^{-1} confirms the presence of para-substituted aniline rings. Also, the peak at 1416 cm^{-1} reappears, which corresponds to the presence of structures with a roselike morphology in this solution. The spectra after 3 h have features typical of standard polyaniline.

It needs to be noted that the conductivity of samples increased with the reaction time in the different reaction solutions. We could not measure the conductivity of the 1 h sample in the nonbuffered, nonacidified solution with the Jandel Model RM2 instrument, while the conductivity of the 3 h sample was 1.5×10^{-3} S cm^{-1}, at 5 h up to 3.8×10^{-2} S/cm, and the conductivity of final 20 h product was 7.9×10^{-2} S cm^{-1}. This result is consistent with the EPR spectra. However, we could not obtain the conductivity of 1 and 3 h samples in pH 3 solution (HCl/phhtalate buffer), while the conductivity of the 5 h sample was 9.4×10^{-2} S cm^{-1} and the conductivity of final 20 h product was 2.2×10^{-2} S cm^{-1}, again consistent with the EPR results.

Conclusions

The oxidative polymerization of aniline in the presence of different buffered solutions (citric acid/phosphate, HCl/phthalate) and nonbuffered solutions has been studied. The morphology of the products in the early stages of the reaction depended significantly on the buffer solution used. However, the final products obtained after 20 h, no matter which solution was employed, were polyaniline nanotubes. The following conclusions can thus be made:

First, in the cases of the oxidative polymerization of aniline in nonbuffered aqueous solution, HCl/phthalate buffer pH 3, citric acid/Na_2HPO_4 buffer pH 3 and pH 4, and in the acidified (HCl/KCl) pH 2 solution, the initial reaction products contained ortho-coupled aniline and phenazine-like structures, revealed by FT-IR peaks at 860 and 1416 cm^{-1}. These products show roselike morphology and, based on the EPR experiment, do not contain charge carriers.

Second, in the case of the pH 3 citric acid/Na_2HPO_4 buffer, the products at the early stage of the reaction presented a bent tapelike morphology, and its FT-IR spectrum did not show the 860 and 1416 cm^{-1} peaks. This result confirms that proposition that these peaks are indicative of the roselike morphology and nonconductive aniline oxidative products as well as the fact that not only the pH but also the solution composition (the nature of the buffer) determines the nature of the reaction products.

Third, products of the aniline oxidation at longer reaction times (5−20 h) in all the investigated cases revealed that the presence of FT-IR peaks at 824 cm^{-1} (para-coupling of aniline) and 1141 cm^{-1} ($-NH^+$ indicative of conductive PANI) and complete nanotubular PANI morphology. EPR experiments confirmed their highly conductive nature.

Acknowledgment. The authors gratefully acknowledge the University of Auckland Research Committee grant of a Postdoctoral Fellowship (No. 3606261). Also, the authors acknowledge the New Zealand Foundation for Science and Technology for financial support for this work (New Economy Research Fund, Contract UOAX0408).

References and Notes

(1) Heeger, A. J. *Angew. Chem., Int. Ed.* **2001**, *40*, 2591.
(2) Kaner, R. B.; Baker, C. O.; Kojima, R.; Li, D.; Tran, H.; Shabnam, V.; Weiller, B. H. Abstracts, 40th Western Regional Meeting of the American Chemical Society, Anaheim, CA, Jan 22−25, 2006, WRM.
(3) Virji, S.; Huang, J.; Kaner, R. B.; Weiller, B. H. *Nano Lett.* **2004**, *4*, 491.
(4) Zhang, L.; Peng, H.; Kilmartin, P. A.; Soeller, C.; Travas-Sejdic, J. *Electroanalysis* **2007**, *19*, 870.
(5) Martin, C. R. *Science* **1994**, *266*, 1961.
(6) Li, M.; Guo, Y.; Wei, Y.; MacDiarmid, A. G.; Lelkes, P. I. *Biomaterials* **2006**, *27*, 2705.
(7) Zhang, X.; Goux, W. J.; Manohar, S. K. *J. Am. Chem. Soc.* **2004**, *126*, 4502.
(8) He, Y. *Appl. Surf. Sci.* **2006**, *252*, 2115.
(9) Guan, F.; Chen, M.; Yang, W.; Wang, J.; Zhang, R.; Yang, S.; Xue, Q. *Colloids Surf., A* **2005**, *117*, 257–258.
(10) Wan, M.; Wei, Z.; Zhang, Z.; Zhang, L.; Huang, K.; Yang, Y. *Synth. Met.* **2003**, *175*, 135–136.
(11) Wan, M.; Li, J. *J. Polym. Sci., Part A: Polym. Chem.* **2000**, *38*, 2359.
(12) Trchova, M.; Sedenkova, I.; Konyushenko, E. N.; Stejskal, J.; Holler, P.; Ciric-Marjanovic, G. *J. Phys. Chem. B* **2006**, *110*, 9461.
(13) Wei, Z.; Zhang, Z.; Wan, M. *Langmuir* **2002**, *18*, 917.
(14) Zhang, L.; Wan, M. *Nanotechnology* **2002**, *13*, 750.
(15) Zhang, L.; Wan, M. *Adv. Funct. Mater.* **2003**, *13*, 815.
(16) Zhang, L.; Long, Y.; Chen, Z.; Wan, M. *Adv. Funct. Mater.* **2004**, *14*, 693.
(17) Zhang, L.; Wan, M.; Wei, Y. *Macromol. Rapid Commun.* **2006**, *27*, 888.
(18) Zhang, Z.; Wei, Z.; Wan, M. *Macromolecules* **2002**, *35*, 5937.
(19) Zhang, Z.; Wei, Z.; Zhang, L.; Wan, M. *Acta Mater.* **2005**, *53*, 1373.
(20) Wei, Z.; Zhang, L.; Yu, M.; Yang, Y.; Wan, M. *Adv. Mater.* **2003**, *15*, 1382.
(21) Zhang, L.; Zhang, L.; Wan, M.; Wei, Y. *Synth. Met.* **2006**, *156*, 454.
(22) Zhang, L.; Wan, M. *Adv. Funct. Mater.* **2003**, *13*, 815.
(23) Zhang, L.; Peng, H.; Zujovic, Z. D.; Kilmartin, P. A.; Travas-Sejdic, J. *Macromol. Chem. Phys.* **2007**, *208*, 1210.
(24) Shen, Y.; Sun, J.; Wu, J.; Zhou, Q. *J. Appl. Polym. Sci.* **2005**, *96*, 814.
(25) Moraes, S. R.; Huerta-Vilca, D.; Motheo, A. J. *Eur. Polym. J.* **2004**, *40*, 2033.
(26) Thiyagarajan, M.; Kumar, J.; Samuelson, L. A.; Cholli, A. L. *J. Macromol. Sci., Pure Appl. Chem.* **2003**, *A40*, 1347.
(27) Brett, C. M. A.; Brett, A. M. C. F. O.; Pereira, J. L. C.; Rebelo, C. *J. Appl. Electrochem.* **1993**, *23*, 332.
(28) Moraes, S. R.; Huerta-Vilca, D.; Motheo, A. J. *Prog. Org. Coat.* **2003**, *48*, 28.
(29) Moraes, S. R.; Huerta-Vilca, D.; Motheo, A. J. *Mol. Cryst. Liq. Cryst. Sci. Technol., Sect. A* **2002**, *374*, 391.
(30) Konyushenko, E. N.; Stejskal, J.; Sedenkova, I.; Trchova, M.; Sapurina, I.; Cieslar, M.; Prokes, J. *Polym. Int.* **2006**, *55*, 31.
(31) Ding, H.; Shen, J.; Wan, M.; Chen, Z. *Macromol. Chem. Phys.* **2008**, *209*, 864.
(32) Cotarelo, M. A.; Huerta, F.; Quijada, C.; Mallavia, R.; Vazquez, J. L. *J. Electrochem. Soc.* **2006**, *153*, D114.
(33) Stejskal, J.; Sapurina, I.; Trchova, M.; Konyushenko, E. N.; Holler, P. *Polymer* **2006**, *47*, 8253.
(34) Stejskal, J.; Sapurina, I.; Trchova, M.; Konyushenko, E. N. *Macromolecules* **2008**, *41*, 3530.

MA801728J